

Global expansion of covid19 pandemic is driven by population size and airport connections

Marco Tulio Pacheco Coelho ^{Corresp., 1}, **João Fabrício Mota Rodrigues** ¹, **Anderson Matos Medina** ², **Paulo Scalco** ³, **Levi Carina Terribile** ⁴, **Bruno Vilela** ², **José Alexandre Felizola Diniz-Filho** ¹, **Ricardo Dobrovolski** ²

¹ Departamento de Ecologia, Universidade Federal de Goiás, Goiânia, GO, Brazil

² Instituto de Biologia, Universidade Federal da Bahia, Salvador, BA, Brazil

³ Faculdade de Administração, Economia, Ciências Contábeis (FACE), Universidade Federal de Goiás, Goiânia, GO, Brasil

⁴ Laboratório de Macroecologia, Universidade Federal de Jataí, Jataí, GO, Brasil

Corresponding Author: Marco Tulio Pacheco Coelho
Email address: marcotpcelho@gmail.com

The pandemic state of COVID-19 caused by the SARS CoV-2 put the world in quarantine, led to hundreds of thousands of deaths and is causing an unprecedented economic crisis. However, COVID-19 is spreading in different rates at different countries. Here, we tested the effect of three classes of predictors, i.e., socioeconomic, climatic and transport, on the rate of daily increase of COVID-19 on its exponential phase. We found that population size and global connections, represented by countries' importance in the global air transportation network, are the main explanations for the early growth rate of COVID-19 in different countries. Climate and socioeconomics had no significant effect in this big picture analysis. Our results indicate that the current claims that the growth rate of COVID-19 may be lower in warmer and humid countries should be taken very carefully, risking to disturb well-established and effective policy of social isolation that may help to avoid higher mortality rates due to the collapse of national health systems.

1 **Global expansion of covid19 pandemic is driven by population size**
2 **and airport connections**

3

4 Marco Túlio Pacheco Coelho¹, João Fabricio Mota Rodrigues¹, Anderson Matos
5 Medina², Paulo Scalco³, Levi Carina Terribile⁴, Bruno Vilela², José Alexandre
6 Felizola Diniz-Filho¹ & Ricardo Dobrovolski²

7

8 *1 Departamento de Ecologia, Universidade Federal de Goiás, Goiânia, Goiás, Brazil.*

9 *2 Instituto de Biologia, Universidade Federal da Bahia, Salvador, BA, Brazil*

10 *3. Faculdade de Administração, Economia, Ciências Contábeis (FACE), Universidade Federal*
11 *de Goiás, Goiânia, Goiás, Brazil.*

12 *4. Laboratório de Macroecologia, Universidade Federal de Jataí, Jataí, GO, Brazil*

13

14

15 Corresponding Author:

16 Marco Túlio Pacheco Coelho

17 Departamento de Ecologia, Universidade Federal de Goiás, Goiânia, Goiás, Brazil

18 e-mail: marcotpcoelho@gmail.com

19

20

22 Abstract

23 The pandemic state of COVID-19 caused by the SARS CoV-2 put the world in
24 quarantine, led to hundreds of thousands of deaths and is causing an unprecedented economic
25 crisis. However, COVID-19 is spreading in different rates at different countries. Here, we tested
26 the effect of three classes of predictors, i.e., socioeconomic, climatic and transport, on the rate of
27 daily increase of COVID-19 on its exponential phase. We found that population size and global
28 connections, represented by countries' importance in the global air transportation network, are
29 the main explanations for the early growth rate of COVID-19 in different countries. Climate and
30 socioeconomics had no significant effect in this big picture analysis. Our results indicate that the
31 current claims that the growth rate of COVID-19 may be lower in warmer and humid countries
32 should be taken very carefully, risking to disturb well-established and effective policy of social
33 isolation that may help to avoid higher mortality rates due to the collapse of national health
34 systems.

35

36

37 **Introduction**

38 With the worldwide spread of the novel Coronavirus Disease 2019 (COVID-19), caused
39 by the SARS-CoV-2 virus, we are experiencing a declared pandemic. One of the largest
40 preoccupations about this new virus is its notable ability to spread given the absence of any
41 effective treatment, vaccine, and immunity in human populations. Epidemiologists quantify the
42 ability of infectious agents to spread by estimating the basic reproduction number (R_0) statistic
43 (Delamater et al., 2019), which measures the average number of people each contagious person
44 infects. The new coronavirus is transmitting at an average R_0 between 2.7 and 3.2 (Billah et al.
45 2020, Liu et al. 2020), which is greater than seasonal influenza viruses that spread every year
46 around the planet (median R_0 of 1.28, Biggerstaff et al., 2014). To anticipate the timing and
47 magnitude of public interventions and mitigate the adverse consequences on public health and
48 economy, understanding the factors associated with the survival and transmission of SARS-CoV-
49 2 is urgent.

50 Because previous experimental (Lowen et al., 2007), epidemiological (Shaman et al.,
51 2010, Barreca & Shimshack 2012), and modeling (Zuk et al., 2009) studies show the critical
52 role of temperature and humidity on the survival and transmission of viruses, recent studies are
53 testing the effect of environmental variables on SARS-CoV-2 (Wang et al., 2020, Sajadi et al.,
54 2020, Harbert et al. 2020, Araújo et al. 2020) and forecasting monthly scenarios of the spread of
55 the new virus based on climate suitability (Araújo & Naimi 2020, *but see* Carlson et al. 2020).
56 Although temperature and humidity affect the spread and survival of other coronaviruses (i.e.,
57 SARS-CoV and MERS-CoV, Tan et al., 2005, Chan et al., 2011, Doremalen et al., 2013, Gaunt
58 et al., 2010) using the current occurrences of SARS-CoV-2 cases to build correlative climatic
59 suitability models without considering connectivity among different locations and

60 socioeconomic conditions might be inadequate, especially considering that the definition of
61 climatic niche of a respiratory virus, transmitted from person to person, is very challenging
62 (Carlson et al. 2020).

63 Many factors might influence the distribution of diseases at different spatial scales.
64 Climate might affect the spread of viruses given its known effect on biological processes that
65 influences many biogeographical patterns, including the distribution of diseases and human
66 behavior (e.g., Murray et al., 2018). Geographic distance represents the geographical space
67 where the disease spread following the distribution of hosts and also explains biogeographic
68 patterns (Pulin 2003, Nekola & White 2004, Warren 2014). Socioeconomic characteristics of
69 countries include population size, which represent a key epidemiological parameter that
70 determines the rate and reach of pandemics (Grassly & Fraser 2008) and other variables that
71 represent a proxy for the ability to identify and treat infected people and for the governability
72 necessary to make fast political decision and avoid the spread of new diseases (Adler & Newman
73 2003, Gilbert et al. 2020, Khalatbari-Soltani et al. 2020). Finally, the global transportation
74 network might surpass other factors as it can reduce the relative importance of geographic
75 distance and facilitate the spread of viruses and their vectors (Brockmann & Helbing 2013,
76 Pybus et al., 2015). According to the International Air Transport Association (2019) more than 4
77 billion passengers made international travels in 2018. This amount of travelers reaching most of
78 our planet's surface represents a human niche construction (Boivin et al., 2016) that facilitates
79 the global spread of viruses and vectors (Brockmann & Helbing 2013) in the same way it
80 facilitated the spread of invasive species and domesticated animals over modern human history
81 (Boiving et al., 2016).

82 The spread of SARS-CoV-2 from central China to other locations might be strongly
83 associated with inter-country connections, which might largely surpass the effect of climate
84 suitability. Thus, at this point of the pandemic, there is still a distributional disequilibrium that
85 can generate very biased predictions based on climatic correlative modeling (De Marco et al.,
86 2008). Here we used an alternative macroecological approach (Burnside et al., 2012), based on
87 the geographical patterns of early growth rates of the disease at country level, to investigate the
88 drivers of the growth rates of COVID-19 in its exponential phase. We studied the effect of
89 environment, socioeconomic, and global transportation controlling for spatial autocorrelation
90 that could bias model significance. By analyzing these factors, we show that the exponential
91 growth rate of COVID-19 at global scale is explained mainly by population size and country's
92 importance in the global transportation network.

93

94 **Material & Methods**

95 We collected the number of detected cases of COVID-19 per day from the John Hopkins
96 (Dong et al., 2020) and European Centre for Disease Prevention and Control (ECDC, 2020). For
97 each country we only used the “exponential” portion of the time series data (i.e. number of new
98 people infected per day) and excluded days after stabilization or decrease in total number of
99 cases (e.g. Fig S1). Although we are aware that more complex logistic-like curves of growing
100 cases are expected, simpler exponential growth rates are a simpler description of the expansion
101 in early phases and in practice coefficients are indistinguishable from logistic when $N \ll K$. This
102 procedure is also important to guarantee that only the early phase of the disease is analysed given
103 that stabilization and decreasing in growth rates are caused both by natural population dynamics
104 (following a logistic model) and by the interplay of different interventions made by each country,

105 such as political and legal reinforcements of social distancing measures, including lockdown,
106 obligatory mask use and others (Chinazzi et al. 2020, Kraemer et al. 2020, Zhang et al. 2020).
107 Time series data are available for 204 countries, for which 65 had more than 100 cases recorded
108 and for which time series had at least 30 days of exponential growth after the 100th case. We also
109 performed the analysis considering countries with more than 50 cases, but it did not qualitatively
110 change our results. Thus, we only show the results for countries with more than 100 cases.

111 We empirically modelled each time series using an exponential growth model for each
112 country and calculated both the intrinsic growth rate (r) and the regression coefficient of the log
113 growth series to be used as the response variable in our models. Because both were highly
114 correlated (Pearson's $r = 0.97$, Fig S2), we used only the regression coefficient to represent the
115 growth rate of COVID-19 in our study.

116 To investigate potential correlates of the virus growth rate, we downloaded climatic and
117 socioeconomic data of each country. We used climatic data represented by monthly average
118 minimum and maximum temperature ($^{\circ}\text{C}$) and total precipitation (mm) retrieved from the
119 WorldClim database (<https://www.worldclim.org>) (Fick & Hijmans 2017). We used monthly
120 data for 2018, the most recent year available in WorldClim (Fick & Hijmans 2017, Harris et al.
121 2014). We extracted climatic data from the months of January, February, March, and December
122 to represent the climatic conditions of the winter season in the Northern Hemisphere and the
123 summer season in the Southern Hemisphere. Temperature and precipitation are used here
124 because of their critical role on virus transmissions (Lowen et al., 2007, Shaman et al., 2010,
125 Barreca & Shimshack 2012, Zuk et al., 2009) and because of the recent investigations about its
126 potential effect on the spread of COVID-19 (Araújo & Naimi 2020, Harbert et al. 2020). In
127 addition, the predefined time period, winter in the northern hemisphere and summer in the

128 southern hemisphere, represents the seasons in which the virus started to spread in the different
129 hemispheres. From these data, we computed the mean value of climatic variables across each
130 country. Finally, minimum, and maximum temperatures were combined to estimate monthly
131 mean temperature for December, January, February, and March, which was used in the model
132 along with total precipitation for the same months. However, using different combinations of
133 these variables (i.e., using means of minimum or maximum temperatures, as well as minimum or
134 maximum for each month) did not qualitatively affect our results.

135 We extracted socioeconomic data for each country. Human Development Index (HDI)
136 rank, mean number of school years in 2015, gross national income (GNI) per capita in 2018
137 population size in 2015 and average annual population growth rate between 2010-2015 were
138 used in our study and downloaded from the United Nations database
139 (<http://hdr.undp.org/en/data>) and from the World Inequality Database (<https://wid.world>). We
140 also obtained a mean value of investments in health care by averaging the annual investments in
141 health care in each country between 2005-2015 obtained from the World Health Organization
142 database (<http://apps.who.int/gho/data/node.home>). Due to the strong collinearity among some of
143 these predictors, HDI rank and mean number of school years were removed from our final
144 model.

145 Finally, we also downloaded air transportation data from the OpenFlights (2014) database
146 regarding the airports of the world, which informs where each airport is located including
147 country location (7,834 airports), and whether there is a direct flight connecting the airports
148 (67,663 connections). We checked the Openflights database to make the airports and connections
149 compatible by including missing or fixing airport codes and removing six unidentified airport
150 connections resulting in a total of 7,834 airports and 67,657 connections. We used this

151 information to build an air transportation network that reflects the existence of a direct flight
152 between the airports while considering the direction of the flight. Thus, the airport network is a
153 unipartite, binary, and directed graph where airports are nodes and flights are links (Fig 1, Fig
154 S3). In the following step, we collapsed the airports' network into a country-level network using
155 the country information to merge all the airports located in a country in a single node (e.g.,
156 United States had 613 airports that were merged in a single vertex representing the country). The
157 country-level network (Fig 1, Fig S3) is a directed weighted graph where the links are the
158 number of connections between 226 countries which is collapsed for the 65 countries that had
159 more than 100 cases and for which time series data had at least 30 days after the 100th case .
160 Afterward, we measured the countries centrality in the network using the Eigenvector Centrality
161 (Bonacich, 1987), that weights the importance of a country in the network considering the
162 number of connections with other countries and how well connected these countries are to other
163 countries – indirect connections. All networks analyses were generated using package *igraph*
164 (Csardi & Nepusz, 2006).

165 We evaluated the relationship between the predictors (climatic, socioeconomic and
166 transport data) and our growth rate parameter (the regression coefficient of the log-transformed
167 growth series) using a standard multiple regression (OLS) considering the distribution of the
168 original predictors as well as the normality of residuals. Moreover, OLS residuals were
169 inspected to evaluate the existence of spatial autocorrelation that could upward bias the
170 significance of predictor variables on the model using Moran's correlograms (Legendre &
171 Legendre 2013). Prior to the analysis, we applied logarithmic (mean precipitation, total
172 population size, and network centrality) and square root (mean health investments)
173 transformations to the data to approximate a normal distribution.

174

175 Results

176 The models used to estimate COVID-19 growth rate on different countries showed an
177 average R^2 of 0.91 (SD = 0.04), varying from 0.78 to 0.99, indicating an overall excellent
178 performance on estimating growth rates. The geographical patterns in the growth rates of
179 COVID-19 cases do not show a clear trend, at least in terms of latitudinal variation, that would
180 suggest a climatic effect at macroecological scale (Fig. 2).

181 We build one model including only climate, which explained only 0.03% of the variation
182 on growth rates. When we added socioeconomic variables, the R^2 increased to 53.95%. Finally,
183 when we added country centrality (i.e. country importance in the global transportation network)
184 as a predictor, the R^2 increased to 59.56%. In this model, only population size and country
185 centrality had positive and significant effects (Fig 3, Table 1). Thus, exponential growth rates
186 increased *strongly* in response to countries population size and their importance in the
187 transportation network (Table 1, Fig 3). Statistical coefficients were not upward biased by spatial
188 autocorrelation.

189

190 Discussion

191 At global scale, Gross National Income, annual population growth, investment in
192 healthcare, mean temperature and mean precipitation had no significant effect on the exponential
193 phase of COVID-19. Population size and countries importance in the global transportation
194 network have key roles on the growth rate of COVID-19.

195 Population size is a critical factor in epidemiological outbreaks and faster growths of
196 COVID-19 were reported in cities with larger populations (Stier et al. 2020). Here, we observe

197 the same pattern at country level. Faster spread in regions with larger populations have been
198 explained by the interaction of frequent trades and people exchanges, and the difficulty to control
199 early outbreaks within larger populations (Jaffe et al. 2020, Harbert et al. 2020, Stier et al. 2020).
200 Because of the multiple infection routes and faster spread in larger populations, recent
201 discussions emphasize the need to implement more aggressive social distancing policies in
202 regions with larger populations (Stier et al. 2020). However, not only population size explains
203 the exponential growth of COVID-19 in different countries but also how central a country is in
204 the global transportation network.

205 Network centrality measures are widely used to discover distinguished nodes on
206 networks, including epidemiological networks (e.g., Madotto & Liu 2016). Our findings
207 reinforce the importance of propagule pressure on disease dissemination (Tian et al., 2017,
208 Chinazzi et al., 2020). Aerial transportation is an important predictor of COVID-19
209 dissemination in China (Kraemer et al., 2020), Brazil (Ribeiro et al., 2020), and Mexico (Dáttilo
210 et al., 2020). Countries characterized by higher centrality in the global transportation network
211 represent distinguished nodes, in terms of how well they are directly and indirectly connected to
212 other countries. These countries are the ones that are more prone to receive higher number of
213 infected individuals in different regions of their territory, which can potentially contribute to the
214 velocity of the initial spread of the disease.

215 The rapid international spread of the severe acute respiratory syndrome (SARS) from
216 2002 to 2003 led to extensively assessing entry screening measures at international borders of
217 some countries (Bell et al., 2003, John et al., 2017). However, it is important to note that SARS-
218 CoV-2 can spread from pre-symptomatic and asymptomatic individuals (Gandhi et al. 2020, Bai
219 et al. 2020). Thus, entry screening measures at international borders might be only partially

220 effective to identify symptomatic individuals, but not effective to stop de disease at international
221 borders. Even for diseases that could be stopped by identifying symptomatic travellers, there is
222 no consensus of the effective and accurate tools to be used in airports across the globe (Sun et al.,
223 2017). Finally, how effective airports closures were in different countries to decrease or stabilize
224 the spread of COVID-19 still needs to be tested in different countries and is beyond the scope of
225 this paper. However, after local transmissions are identified, we would expect that airport
226 closures are less effective than any other measure taken by governments, such as increasing
227 social distancing, tracking and isolating infected individuals (see Chinazzi et al. 2020).

228 When discussing and modelling the effect of climate on SARS CoV-2 it is important to
229 remember that modern human society is a complex system composed by strongly connected
230 societies that are all susceptible to rare events. It is also critical to consider the negative
231 correlations between climate and local or regional socioeconomic conditions (i.e., inadequate
232 sanitary conditions and poor nutritional conditions) that could easily counteract any potential
233 climatic effect at local scales, such as lower survival rates of viruses exposed to high humidity,
234 temperatures and high UV irradiation (Wang et al., 2020, Duan et al., 2003). Our analyses call
235 attention to the case of Brazil, a well-connected and populated tropical country that presents one
236 of the highest increase rates of COVID-19 in its exponential phase. If decision makers consider
237 yet unsupported claims that growth rates of COVID-19 in its exponential phase might be lower
238 in warmer and humid countries, we might observe terrible scenarios unrolling in well-connected
239 and populated countries independent of their climatic conditions.

240

241 **Conclusions**

242 Here, we show that countries' population size and importance in the global transportation
243 network have key roles on the initial growth rate of COVID-19. We do not expect that our results
244 using a macroecological approach at a global scale would have a definitive effect on decision-
245 making in terms of public health in any particular country, province, or city.

246 However, we call the attention for the absence of effects of climatic variables on the
247 exponential phase of COVID-19 that is surpassed by how distinguished a country is in the air
248 transportation network and by their population size. Thus, claims that the growth of COVID-19
249 might be lower in warmer and humid countries based on climate suitability models should be
250 taken very carefully, risking to disturb well-established and effective policy of social isolation
251 that may help to avoid higher mortality rates due to the collapse in national health systems.

252

253 **Acknowledgments**

254 This paper was developed in the context of the human macroecology project in the National
255 Institute of Science and Technology (INCT) in Ecology, Evolution and Biodiversity
256 Conservation, supported by CNPq (grant 465610/2014-5) and FAPEG (grant
257 201810267000023). JAFDF, RD, LCT are also supported by CNPq productivity scholarships.
258 We thank Thiago F. Rangel, André Menegotto, Robert D. Morris, Marcus Cianciaruso, Diogo
259 Proverte and Blas M. Benito for their constructive comments on the manuscript.

260

261

262 **References**

263

264

265 Adler NE, Newman K. 2002. Socioeconomic disparities in health: Pathways and policies. *Health*
266 *Affairs* 21:60–76. DOI: 10.1377/hlthaff.21.2.60.

- 267
268 Araujo MB, Naimi B. 2020 Spread of SARS-CoV-2 Coronavirus likely to be constrained by
269 climate. *medRxiv*, 2020.03.12.20034728. (doi:10.1101/2020.03.12.20034728)
270
- 271 Bai Y, Yao L, Wei T, Tian F, Jin D-Y, Chen L, Wang M. 2020. Presumed Asymptomatic Carrier
272 Transmission of COVID-19. *JAMA* 323:1406–1407. DOI: 10.1001/jama.2020.2565.
273
- 274 Barreca AI, Shimshack JP. 2012 Absolute humidity, temperature, and influenza mortality: 30
275 years of county-level evidence from the united states. *Am. J. Epidemiol.* **176**, 114–122.
276 (doi:10.1093/aje/kws259)
277
- 278 Bell DM *et al.* 2004 Public health interventions and SARS spread, 2003. *Emerg. Infect. Dis.* **10**,
279 1900–1906. (doi:10.3201/eid1011.040729)
280
- 281 Biggerstaff M, Cauchemez S, Reed C, Gambhir M, Finelli L. 2014 Estimates of the reproduction
282 number for seasonal, pandemic, and zoonotic influenza: A systematic review of the
283 literature. *BMC Infect. Dis.* **14**, 1–20. (doi:10.1186/1471-2334-14-480)
284
- 285 Billah MA, Miah MM, Khan MN. 2020. Reproductive number of COVID-19: A systematic
286 review and meta-analysis based on global level evidence. *medRxiv*:2020.05.23.20111021.
287 DOI: 10.1101/2020.05.23.20111021.
288
- 289 Bitar D. , Goubar A. DJC. 2009 International travels and fever screening during epidemics: a
290 literature review on the effectiveness and potential use of non-contact infrared
291 thermometers. *Euro Surveill* **14**, pii=19115.
292
- 293 Boivin NL, Zeder MA, Fuller DQ, Crowther A, Larson G, Erlandson JM, Denhami T, Petraglia
294 MD. 2016 Ecological consequences of human niche construction: Examining long-term
295 anthropogenic shaping of global species distributions. *Proc. Natl. Acad. Sci. U. S. A.* **113**,
296 6388–6396. (doi:10.1073/pnas.1525200113)
297
- 298 Bonacich P. 1987 Power and Centrality: A Family of Measures. *Am. J. Sociol.* **92**, 1170–1182.
299 (doi:10.1086/228631)
- 300 Brockmann D, Helbing D. 2013 The hidden geometry of complex, network-driven contagion
301 phenomena. *Science (80)*. **342**, 1337–1342. (doi:10.1126/science.1245200)
302
- 303 Burnside WR, Brown JH, Burger O, Hamilton MJ, Moses M, Bettencourt LMA. 2012 Human
304 macroecology: linking pattern and process in big-picture human ecology. *Biol. Rev.* **87**,
305 194–208. (doi:10.1111/j.1469-185X.2011.00192.x)
306
- 307 Carlson CJ, Chipperfield JD, Benito BM, Telford RJ, O’Hara RB. 2020. Species distribution
308 models are inappropriate for COVID-19. *Nature Ecology and Evolution* 4:770–771. DOI:
309 10.1038/s41559-020-1212-8.
310
311

- 312 Chan KH, Peiris JSM, Lam SY, Poon LLM, Yuen KY, Seto WH. 2011 The effects of
313 temperature and relative humidity on the viability of the SARS coronavirus. *Adv. Virol.*
314 **2011**. (doi:10.1155/2011/734690)
315
- 316 Chinazzi M, Davis JT, Ajelli M, Gioannini C, Litvinova M, Merler S, Pastore Y Piontti A, Mu
317 K, Rossi L, Sun K, Viboud C, Xiong X, Yu H, Halloran ME, Longini IM, Vespignani A.
318 2020. The effect of travel restrictions on the spread of the 2019 novel coronavirus
319 (COVID-19) outbreak. *Science (New York, N.Y.)* 9757:1–12. DOI:
320 10.1126/science.aba9757.
321
- 322 Csardi G, Nepusz T .2006. The igraph software package for complex network
323 research. *InterJournal, Complex Systems*, 1695. <http://igraph.org>.
324
- 325 Dattilo W, Silva AC, Guevara R, McGregor-Fors I, Pontes S. 2020 COVID-19 most vulnerable
326 Mexican cities lack the public health infrastructure to face the pandemic: a new
327 temporally-explicit model. *medRxiv* , 1–13. (doi:10.1101/2020.04.10.20061192)
328
- 329 De Marco P, Diniz-Filho JAF, Bini LM. 2008 Spatial analysis improves species distribution
330 modelling during range expansion. *Biol. Lett.* **4**, 577–580. (doi:10.1098/rsbl.2008.0210)
331
- 332 Delamater PL, Street EJ, Leslie TF, Yang YT, Jacobsen KH. 2019 Complexity of the basic
333 reproduction number (R0). *Emerg. Infect. Dis.* **25**, 1–4. (doi:10.3201/eid2501.171901)
334
- 335 Dong E, Du H, Gardner L. 2020 An interactive web-based dashboard to track COVID-19 in real
336 time. *Lancet Infect. Dis.* **20**, 533–534. (doi:10.1016/S1473-3099(20)30120-1)
337
- 338 Doremalen NV, Bushmaker T, Munster VJ. 2013 Stability of middle east respiratory syndrome
339 coronavirus (MERS-CoV) under different environmental conditions. *Eurosurveillance*
340 **18**, 1–4. (doi:10.2807/1560-7917.ES2013.18.38.20590)
341
- 342 Duan S-M, Zhao X-S, Wen R-F, Huang J-J, Pi G-H, Zhang S-X, Han J, Bi S-L, Ruan L, Dong
343 X-P. 2003. Stability of SARS coronavirus in human specimens and environment and its
344 sensitivity to heating and UV irradiation. *Biomedical and environmental sciences : BES*
345 **16**:246–255.
346
- 347 Enserink, M & Kupferschmidt, K. (2020). Mathematics of life and death: How disease models
348 shape national shutdowns and other pandemic policies. *Science*
349 (<https://www.sciencemag.org/news/2020/03/mathematics-life-and-death-how-disease-models-shape-national-shutdowns-and-other#>)
350
- 351
- 352 European Centre for Disease Prevention and Control (ECDC). COVID-19 - Situation update –
353 worldwide. Stockholm: ECDC; 1 Apr 2020. Available from:
354 <https://www.ecdc.europa.eu/en/geographical-distribution-2019-ncov-cases>
355

- 356 Fick SE, Hijmans RJ. 2017 WorldClim 2: new 1-km spatial resolution climate surfaces for global
357 land areas. *Int. J. Climatol.* **37**, 4302–4315. (doi:10.1002/joc.5086)
358
- 359 Gaunt ER, Hardie A, Claas ECJ, Simmonds P, Templeton KE. 2010 Epidemiology and clinical
360 presentations of the four human coronaviruses 229E, HKU1, NL63, and OC43 detected
361 over 3 years using a novel multiplex real-time PCR method. *J. Clin. Microbiol.* **48**, 2940–
362 2947. (doi:10.1128/JCM.00636-10)
363
- 364 Gilbert M, Pullano G, Pinotti F, Valdano E, Poletto C, Boëlle PY, D’Ortenzio E, Yazdanpanah
365 Y, Eholie SP, Altmann M, Gutierrez B, Kraemer MUG, Colizza V. 2020. Preparedness
366 and vulnerability of African countries against importations of COVID-19: a modelling
367 study. *The Lancet* 395:871–877. DOI: 10.1016/S0140-6736(20)30411-6.
368
- 369 Grassly NC, Fraser C. 2008. Mathematical models of infectious disease transmission. *Nature*
370 *Reviews Microbiology* 6:477–487. DOI: 10.1038/nrmicro1845.
371
- 372 Harbert RS, Cunningham SW, Tessler M. 2020. Spatial modeling cannot currently differentiate
373 SARS-CoV-2 coronavirus and human distributions on the basis of climate in the United
374 States. *medRxiv*:2020.04.08.20057281. DOI: 10.1101/2020.04.08.20057281.
375
376
- 377 Harris I, Jones PD, Osborn TJ, Lister DH. 2014 Updated high-resolution grids of monthly
378 climatic observations - the CRU TS3.10 Dataset. *Int. J. Climatol.* **34**, 623–642.
379 (doi:10.1002/joc.3711)
380
- 381 International Air Transport Association. 2019. Annual
382 Review([https://www.iata.org/contentassets/c81222d96c9a4e0bb4ff6ced0126f0bb/iata-
383 annual-review-2019.pdf](https://www.iata.org/contentassets/c81222d96c9a4e0bb4ff6ced0126f0bb/iata-annual-review-2019.pdf))
384
- 385 Jaffe R, Vera MPO, Jaffe K. 2020. Globalized low-income countries may experience higher
386 COVID-19 mortality rates. *medRxiv*:2020.03.31.20049122. DOI:
387 10.1101/2020.03.31.20049122.
388
389
- 390 John St. RK, King A, De Jong D, Bodie-Collins M, Squires SG, Tam TWS. 2005 Border
391 screening for SARS. *Emerg. Infect. Dis.* **11**, 6–10. (doi:10.3201/eid1101.040835)
392
- 393 Khalatbari-Soltani S, Cumming RG, Delpierre C, Kelly-Irving M. 2020. Importance of collecting
394 data on socioeconomic determinants from the early stage of the COVID-19 outbreak
395 onwards. *Journal of epidemiology and community health*:620–623. DOI: 10.1136/jech-
396 2020-214297.
397
- 398 Kraemer MUG, Yang CH, Gutierrez B, Wu CH, Klein B, Pigott DM, du Plessis L, Faria NR, Li
399 R, Hanage WP, Brownstein JS, Layan M, Vespignani A, Tian H, Dye C, Pybus OG,
400 Scarpino S V. 2020. The effect of human mobility and control measures on the COVID-

- 401 19 epidemic in China. *Science (New York, N.Y.)* 497:493–497. DOI:
402 10.1126/science.abb4218.
403
404
- 405 Liu Y, Gayle AA, Wilder-Smith A, Rocklöv J. 2020. The reproductive number of COVID-19 is
406 higher compared to SARS coronavirus. *Journal of Travel Medicine* 27:1–4. DOI:
407 10.1093/jtm/taaa021.
408
409
- 410 Legendre P, Lengedre L. Numerical Ecology. Elsevier Science.
411
- 412 Lowen AC, Mubareka S, Steel J, Palese P. 2007 Influenza virus transmission is dependent on
413 relative humidity and temperature. *PLoS Pathog.* 3, 1470–1476.
414 (doi:10.1371/journal.ppat.0030151)
415
- 416 Madotto A, Liu J. 2016 Super-Spreader Identification Using Meta-Centrality. *Sci. Rep.* 6, 1–10.
417 (doi:10.1038/srep38994)
418
- 419 Murray KA, Olivero J, Roche B, Tiedt S, Guégan JF. 2018 Pathogeography: leveraging the
420 biogeography of human infectious diseases for global health management. *Ecography*
421 (*Cop.*). 41, 1411–1427. (doi:10.1111/ecog.03625)
422
- 423 Nekola JC, White PS. 1999 The distance decay of similarity in biogeography and ecology. *J.*
424 *Biogeogr.* 26, 867–878. (doi:10.1046/j.1365-2699.1999.00305.x)
425
- 426 Nishiura H, Kamiya K. 2011 Fever screening during the influenza (H1N1-2009) pandemic at
427 Narita International Airport, Japan. *BMC Infect. Dis.* 11, 1–11. (doi:10.1186/1471-2334-
428 11-111)
429
- 430 Openflights.org database. 2014. <http://openflights.org/data.html>. Accessed 20 March 2020
- 431 Poulin R. 2003 The decay of similarity with geographical distance in parasite communities of
432 vertebrate hosts. *J. Biogeogr.* 30, 1609–1615. (doi:10.1046/j.1365-2699.2003.00949.x)
433
- 434 Pybus OG, Tatem AJ, Lemey P. 2015 Virus evolution and transmission in an ever more
435 connected world. *Proc. R. Soc. B Biol. Sci.* 282, 1–10. (doi:10.1098/rspb.2014.2878)
436
- 437 Ribeiro SP, Dattilo W, Silva AC e, Reis AB, Goes-Neto A, Alcantara L, Giovanetti M, Coura-
438 vital W, Fernandes GW, Azevedo VA. 2020. Severe airport sanitarian control could slow
439 down the spreading of COVID-19 pandemics in Brazil. *medRxiv*:2020.03.26.20044370.
440 DOI: 10.1101/2020.03.26.20044370.
441
442
- 443 Sajadi MM, Habibzadeh P, Vintzileos A, Shokouhi S, Miralles-Wilhelm F, Amoroso A. 2020
444 Temperature and Latitude Analysis to Predict Potential Spread and Seasonality for
445 COVID-19. *SSRN Electron. J.* , 6–7. (doi:10.2139/ssrn.3550308)
446

- 447 Shaman J, Pitzer VE, Viboud C, Grenfell BT, Lipsitch M. 2010 Absolute humidity and the
448 seasonal onset of influenza in the continental United States. *PLoS Biol.* **8**.
449 (doi:10.1371/journal.pbio.1000316)
450
- 451 Stier AJ, Berman MG, Bettencourt LMA. 2020. COVID-19 attack rate increases with city size.
452 *arXiv*.
453
454
- 455 Sun G., Matsui T., Kirimoto T., Yao Y., Abe S. .2017. Applications of Infrared Thermography
456 for Noncontact and Noninvasive Mass Screening of Febrile International Travelers at
457 Airport Quarantine Stations. In: Ng E., Etehadtavakol M. (eds) Application of Infrared to
458 Biomedical Sciences. Series in BioEngineering. Springer, Singapore
459
- 460 Tan J, Mu L, Huang J, Yu S, Chen B, Yin J. 2005 An initial investigation of the association
461 between the SARS outbreak and weather: With the view of the environmental
462 temperature and its variation. *J. Epidemiol. Community Health* **59**, 186–192.
463 (doi:10.1136/jech.2004.020180)
464
- 465 Tian H, Sun Z, Faria NR, Yang J, Cazelles B, Huang S, Xu B, Yang Q, Pybus OG, Xu B. 2017.
466 Increasing airline travel may facilitate co-circulation of multiple dengue virus serotypes
467 in Asia. *PLOS Neglected Tropical Diseases* 11:e0005694. DOI:
468 10.1371/journal.pntd.0005694.
469
470
- 471 Wang J, Tang K, Feng K, Lv W. 2020 High Temperature and High Humidity Reduce the
472 Transmission of COVID-19. *SSRN Electron. J.* , 1–19. (doi:10.2139/ssrn.3551767)
473
- 474 Warren DL, Cardillo M, Rosauer DF, Bolnick DI. 2014 Mistaking geography for biology:
475 inferring processes from species distributions. *Trends Ecol. & Evol.* **29**, 572–580.
476 (doi:10.1016/j.tree.2014.08.003)
477
- 478 World Health Organization. 2020. Statement on the meeting of the International Health
479 Regulations (2005) Emergency Committee regarding the outbreak of novel coronavirus
480 (2019-nCoV). Retrieved from [https://www.who.int/news-room/detail/23-01-2020-
481 statement-on-the-meeting-of-the-international-health-regulations-\(2005\)-emergency-
482 committee-regarding-the-outbreak-of-novel-coronavirus-\(2019-ncov\)](https://www.who.int/news-room/detail/23-01-2020-statement-on-the-meeting-of-the-international-health-regulations-(2005)-emergency-committee-regarding-the-outbreak-of-novel-coronavirus-(2019-ncov))
483
- 484 Zhang R, Li Y, Zhang AL, Wang Y, Molina MJ. 2020. Identifying airborne transmission as the
485 dominant route for the spread of COVID-19. *Proceedings of the National Academy of
486 Sciences*:202009637. DOI: 10.1073/pnas.2009637117.
487
488
- 489 Zuk T, Rakowski F, Radomski JP. 2009 Probabilistic model of influenza virus transmissibility at
490 various temperature and humidity conditions. *Comput. Biol. Chem.* **33**, 339–343.
491 (doi:10.1016/j.compbiolchem.2009.07.005)
492

Figure 1

Air transportation network among 65 countries that had more than 100 cases and for which time series data had at least 30 days after the 100th case.

Different colours represent modules of countries that are more connected to each other. Different sizes of each node represent the growth rate of COVID-19 estimated for each country.

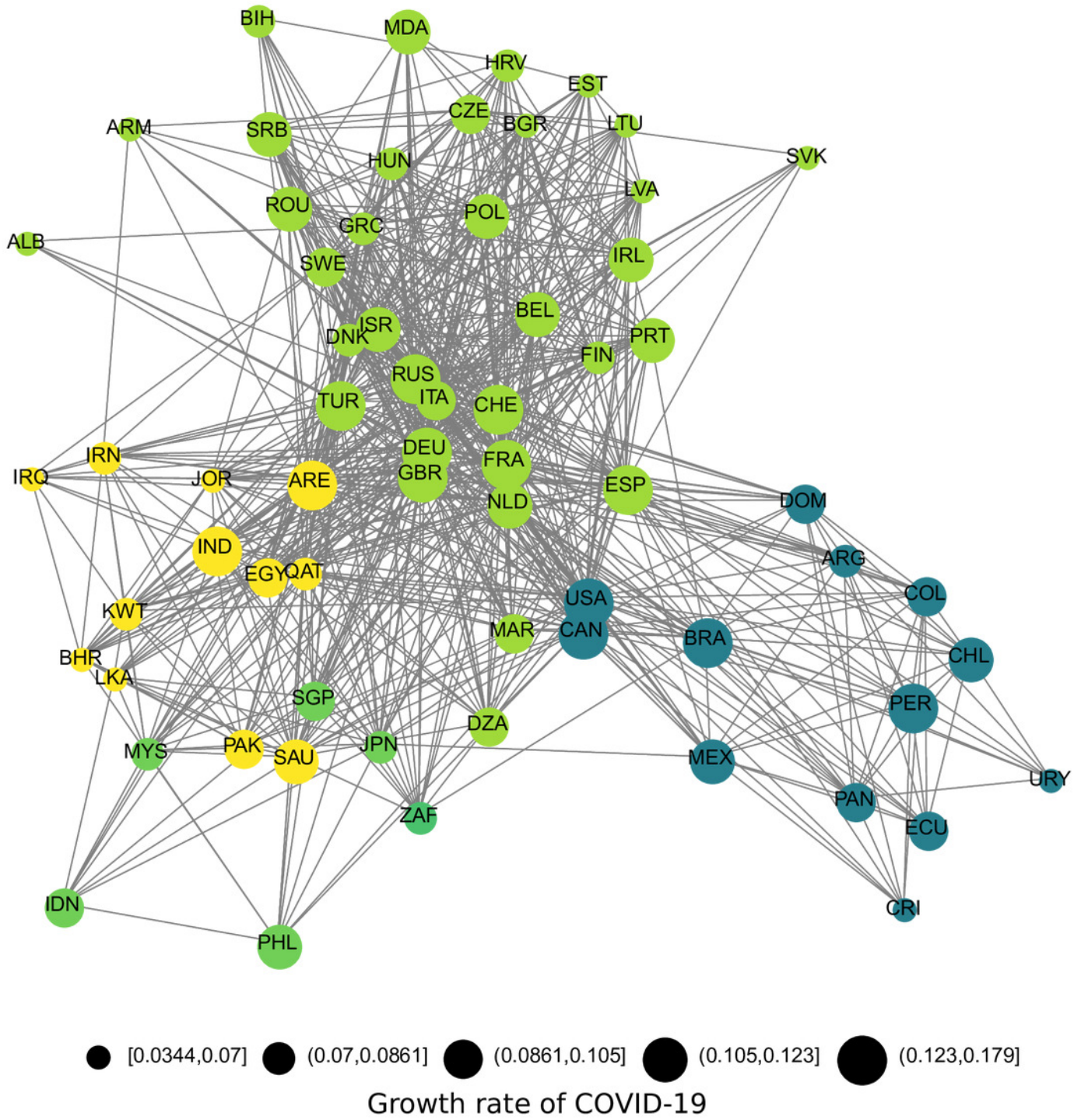


Figure 2

Geographical pattern of the early growth rate of COVID-19 in different countries. Growth rate is represented by the regression coefficient of the log growth series.

Growth Rate

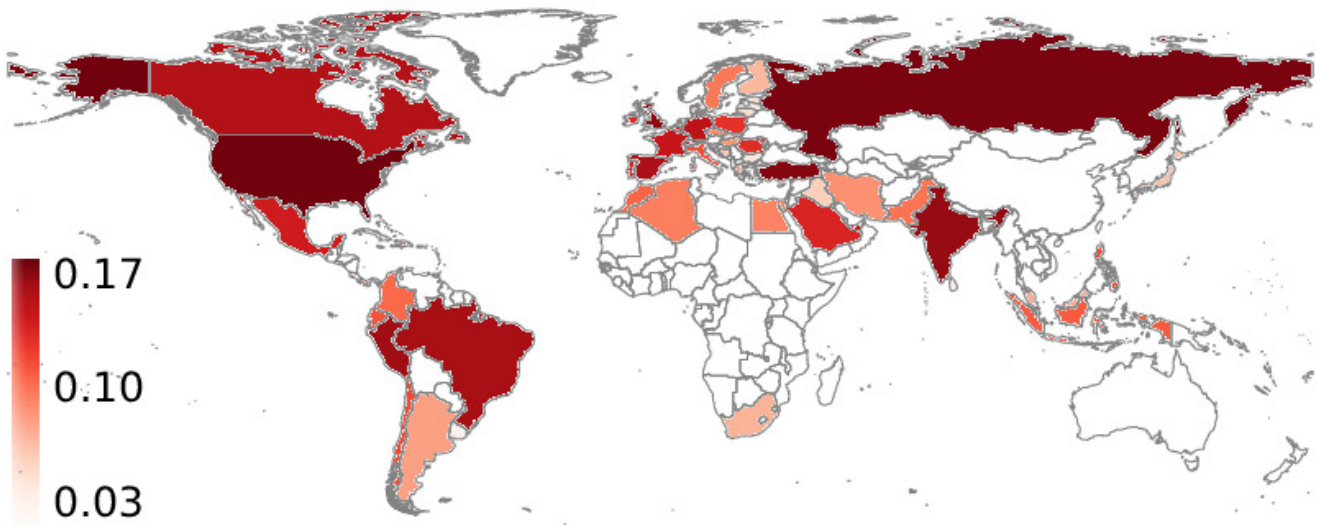
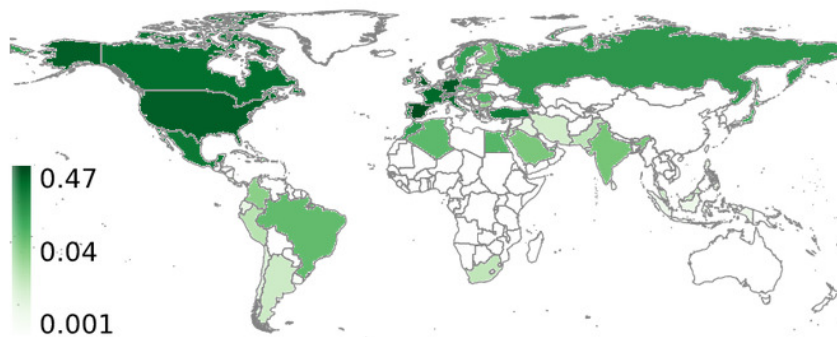


Figure 3

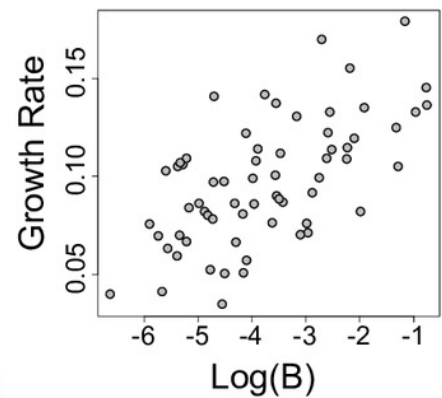
Spatial patterns of predictors and their relationship with COVID-19 growth rates.

Countries importance in the global transportation network (**A**) and population size (**C**) are strongly associated with early growth rates of covid-19 across the world (**B** and **D**).

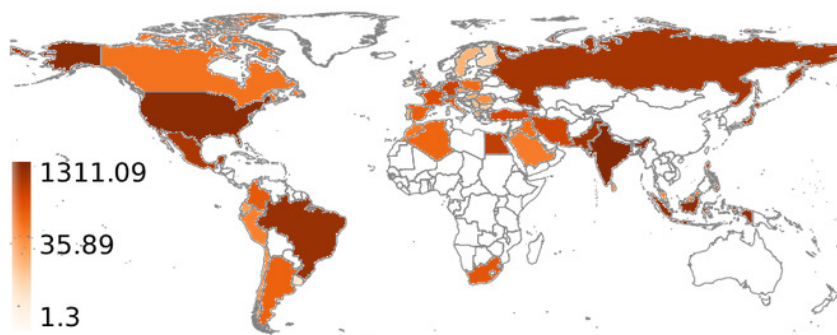
A Eigenvector Centrality



B



C Population Size



D

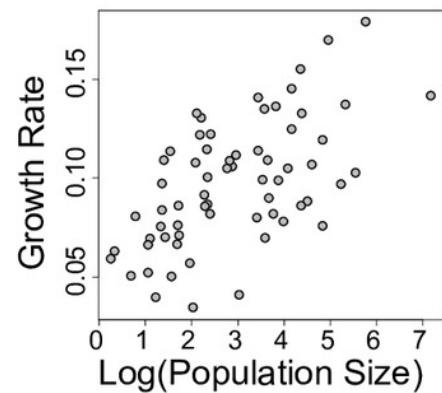


Table 1 (on next page)

Model statistics for all variables used in the study.

1 **Table 1.** Model statistics for all variables used in the study.

	Standardized				
	Estimate	Estimate	Std Error	t value	P-value
<i>Intercept</i>		0.074	0.023	3.232	0.002
<i>Eigenvector Centrality</i>	0.387	0.009	0.003	2.812	0.006
<i>Gross National Income</i>	0.264	0.000	0.000	1.764	0.083
<i>Population Size</i>	0.519	0.011	0.002	4.487	<0.001
<i>Annual population growth</i>	0.096	0.003	0.004	0.658	0.513
<i>Heath investment</i>	-0.168	0.000	0.000	-1.140	0.259
<i>Mean Temperature</i>	-0.208	-0.001	0.000	-1.695	0.095
<i>Mean Precipitation</i>	0.184	0.006	0.003	1.730	0.089

2

3